The International Journal of Cardiovascular Imaging (2020) 36:231–239
https://doi.org/10.1007/s10554-019-01720-8

ORIGINAL PAPER

Comparison of angioscopy and histopathology for the evaluation of carotid plaque characteristics: an ex vivo validation study

Kenji Kawai[1] · Kenichi Fujii[2] · Manabu Shirakawa[3] · Kazutaka Uchida[3] · Kiyofumi Yamada[3] · Rika Kawakami[2] · Takahiro Imanaka[1] · Hiroyuki Hao[4] · Seiichi Hirota[2] · Masaharu Ishihara[1] · Shinichi Yoshimura[3]

Received: 4 May 2019 / Accepted: 18 October 2019 / Published online: 29 October 2019

Abstract

Intravascular angioscopy is widely used for evaluating plaque characteristics through the plaque color in the coronary artery. This study evaluated whether angioscopy is capable of identifying various plaque morphologies, including necrotic core and intraplaque hemorrhage (IPH) in the carotid artery. Nine patients underwent carotid endarterectomy for carotid artery stenosis, and these specimens were imaged ex vivo by angioscopy within 6 h. An angioscopic examination of carotid plaque evaluated its color intensity as follows: white, yellow, or red. The IPH area, necrotic core area, and fibrous cap thickness was measured on histological sections at each site. A total of 7 plaques were graded as white plaques, 10 as yellow, and 8 as red by angioscopy. The IPH area and the percent area occupied by IPH were larger in red and yellow plaques than in white plaques (10.7 ± 9.3 mm^2, 9.4 ± 7.8 mm^2, and 2.2 ± 1.7 mm^2, respectively, $P = 0.074$; and $25 \pm 10\%$, $19 \pm 13\%$, and $7 \pm 5\%$, respectively, $P = 0.008$). Furthermore, the thickness of the fibrous cap was significantly thinner in red plaques than in yellow and white plaques (128 ± 34 µm, 328 ± 136 µm, and 285 ± 102 µm, respectively, $P = 0.002$). The ROC analysis for predicting a presence of red plaques identified that the optimal cutoff value of fibrous cap thickness was 181 µm (area under the curve = 0.987, 100% sensitivity, 90% specificity). The prevalence of red plaques on intravascular angioscopy may represent the existence of plaques containing relatively larger necrotic core and IPH with a thin fibrous cap.

Keywords Carotid artery disease · Atherosclerosis · Angioscopy · Intraplaque hemorrhage · Necrotic core

Abbreviations

ANOVA	Analysis of variance
CCA	Common carotid artery
CEA	Carotid endarterectomy
ICA	Internal carotid artery
IPH	Intraplaque hemorrhage
MRI	Magnetic resonance imaging

✉ Kenichi Fujii
fujiik@hirakata.kmu.ac.jp

[1] Division of Cardiovascular Medicine and Coronary Heart Disease, Hyogo College of Medicine, Nishinomiya, Japan

[2] Department of Surgical Pathology, Hyogo College of Medicine, 1-1 Mukogawa-cho Nishinomiya, Nishinomiya, Hyogo 6638501, Japan

[3] Department of Neurosurgery, Hyogo College of Medicine, Nishinomiya, Japan

[4] Department of Pathology, Nihon University School of Medicine, Tokyo, Japan

Introduction

Approximately one-third of patients admitted with cerebral infarction have significant atherosclerotic stenosis of the ipsilateral carotid artery [1–3]. Although carotid plaque with definite stenosis is subject to carotid endarterectomy (CEA) and carotid artery stenting, carotid plaque composition has been proposed as an important risk factor for stroke [4]. It has been reported that thromboembolic phenomena are associated with thinning and subsequent rupture of the fibrous cap on the surface of atherosclerotic plaques, resulting in release of necrotic debris from the plaque substance [5]. Furthermore, there is increasing evidence that the presence of intraplaque hemorrhage (IPH) in patients with carotid artery stenosis is associated with the development of future ischemic cerebrovascular events [6, 7]. Therefore, assessment and understanding of the carotid plaque characteristics are regarded to be essential before starting treatment for patients with carotid artery stenosis.

Although magnetic resonance imaging (MRI) is one of the most widespread and useful diagnostic tools for

evaluating carotid plaque component at the pre-procedural assessment, it is not able to directly visualize the morphology of the arterial wall. Intravascular angioscopy, a catheter-based technique that can directly visualize the intraluminal morphology and color grade, is a useful tool for understanding plaque characteristics through the plaque color and surface thrombus formation. Plaque color is normally classified as white or yellow according to the surface color of the plaque as seen during angioscopy. This angioscopic color grade assessment is widely performed to evaluate plaque morphology and to predict the clinical prognosis [8–10]. Furthermore, previous studies demonstrated that assessment of coronary tissue characteristics by angioscopy before the procedure could minimize embolic complications during percutaneous coronary intervention [11, 12]. In the present study, we evaluated whether angioscopy is capable of identifying various plaque morphologies, including necrotic core and IPH in the carotid artery by *ex vivo* histological examinations.

Methods

In total, 9 patients underwent CEA for carotid artery stenosis, and these endarterectomy specimens were analyzed. CEA was indicated for > 70% stenosis in symptomatic, and > 50% stenosis in symptomatic cases, according to the North American Symptomatic Carotid Endarterectomy Trial criteria [13]. In 4 patients (44%), lesions were asymptomatic and in 5 (56%) they were symptomatic. A symptomatic lesion was defined as a carotid artery stenosis that had caused ipsilateral ischemic events, including cerebral infarction, transient ischemic attack, and retinal ischemia, within the previous 6 months. The study protocol was approved by the Institutional Review Board of Hyogo College of Medicine, and the study was performed in accordance with regulatory standards and ethical guidelines for clinical studies recommended by the Declaration of Helsinki. All patients provided written informed consent.

CEA procedure

CEA was performed under general anesthesia. After exposing the carotid artery, an intraluminal shunt was inserted in all patients during removing the atherosclerotic plaques. The plaque was extracted in an en bloq fashion. The specimens were stored in 0.9% saline at a temperature of 37 °C for ex vivo imaging by angioscopy, which was performed within 6 h.

Angioscopic examination

Angioscopic images were obtained using a 2.25F angioscopic catheter (Visible; FiberTech, Tokyo, Japan). Before the insertion of the angioscopy catheter, the white balance was adjusted for color correction. The light power was adjusted to avoid reflection and to obtain images with adequate brightness for determination of the plaque color. The angioscopy catheter was carefully inserted from the proximal edge of the common carotid artery (CCA) and advanced to the distal edge of the internal carotid artery (ICA). Subsequently, angioscopy was manually pulled back from the distal edge of the ICA to the proximal edge of the CCA through bifurcation under continuous flush of normal saline. During the angioscopic observation, when only a focal lumen could be observed with a viewing field, we adjusted the direction bias of the angioscopy manually so that the whole circumference of the lumen could be evaluated. Furthermore, when sufficient evaluation could not be conducted with a single pull back, we attempted repeat observation to obtain an adequate angioscopic image of the arterial wall. The acquired images were stored on the system hard drive and processed by offline analysis.

In each section of the ICA, bifurcation, and CCA, which enabled angioscopic observation of the whole circumference, the dominant color tone was evaluated based on the following definitions. White plaque was defined as visually homogeneous white area without color boundaries on the luminal surface (Fig. 1A). Yellow plaque was defined simply as the yellow area on the luminal surface, which have smooth or irregular surface with or without protrusion into the lumen. Red plaques contained red area on the luminal surface of the plaque (Fig. 1B, C). All findings were evaluated by two angioscopic specialists who were blinded to the patient characteristics.

Histological preparation and analysis

The carotid specimens were fixed in 10% neutral-buffered formalin immediately after angioscopic examination. Forty-eight hours after fixation, ring-like arterial specimens obtained at the same level as the imaging study were decalcified for 5 h, embedded in paraffin, and cut every 3 to 4 mm into 4-μm transverse sections perpendicular to the longitudinal axis of the artery. All histological sections were stained with hematoxylin–eosin, elastica van Gieson, and Masson's trichrome. The immunohistochemistry for glycophorin A stain was also performed (1:200 dilution) (Dako, Tokyo, Japan) to identify the IPH. Histological

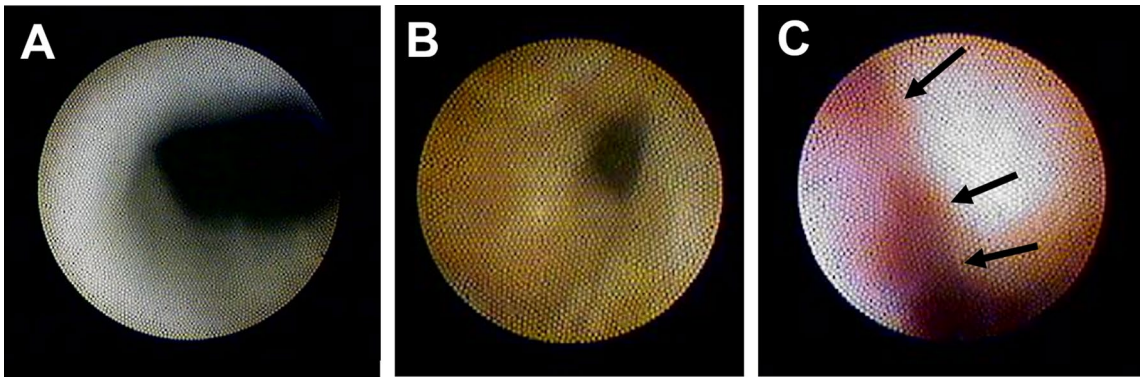

Fig. 1 Representative angioscopic images of a carotid artery. **A** white plaque, **B** yellow plaque, **C** red plaque (arrows)

assessment of each cross-section was performed by a single specialist who was blinded to the imaging results. Quantitative analysis was performed on the histological section using measurement software (ImageJ version 1.44; National Institutes of Health, MD, USA). Measurement parameters were minimum lumen diameter, lumen area, and vessel area. Plaque area was defined as the difference between the vessel area and lumen area. The necrotic core was defined as a hypocellular plaque cavity devoid of collagen and containing necrotic debris and cholesterol clefts. The necrotic core area was measured using measurement software. IPH is defined as a large accumulation of erythrocytes lying free in the tissue [14]. The IPH area was measured as the glycophorin A–positive area. As an index of the degree of histological characteristics, the percentage occupied in plaque area was calculated for the necrotic core and IPH. The thickness of the fibrous cap was measured on Masson's trichrome-stained sections at the site of the thinnest portion.

Statistical analysis

Categorical variables were presented as numbers and percentages. All continuous variables were presented as mean ± standard deviation values. The one-way analysis of variance (ANOVA) was used for comparing continuous variables. Additionally, post-hoc analysis was performed to evaluate variables that were found to be significant by ANOVA. For categorical data, all tests performed were analyzed using chi-square tests or fisher's exact test. Receiver-operating curves (ROCs) were analyzed to assess the best cutoff values of the fibrous cap thickness to determine the presence of red plaques with a maximal accuracy. Difference with $P < 0.05$ was considered significant. All statistical analysis was performed using JMP software version 13.1.0 (SAS Institute Inc., Cary, North Carolina, USA).

Results

In the present study, 9 patients with carotid artery stenosis participated. The patient characteristics are shown in Table 1. All patients received at least one antiplatelet agent at admission. In total, 27 histological sections were matched

Table 1 Baseline characteristics of patients

	N = 9
Gender, male	7 (78)
Age, years	74 ± 4
Symptomatic	6 (67)
Target artery, right/left	5 (56)/4 (44)
Degree of stenosis[a] (%)	68 ± 19
Hypertension	6 (67)
Diabetes mellitus	4 (44)
Dyslipidemia	7 (78)
Smoking	7 (78)
Laboratory variables	
HDL-C (mg/dL)	49 ± 16
LDL-C (mg/dL)	97 ± 21
HbA1c (%)	6.5 ± 0.8
Concomitant medication	
Antiplatelet therapy	9 (100)
Aspirin	6 (67)
Clopidogrel	6 (67)
Cilostazol	2 (22)
Statins	6 (67)
Calcium channel blocker	4 (44)
ACEI/ARB	5 (63)

Values are expressed as mean ± SD or n (%)

HDL-C high-density lipoprotein cholesterol, *LDL-C* low-density lipoprotein cholesterol, *ACEI* indicates angiotensin-converting enzyme inhibitor, *ARB* angiotensin II receptor blocker

[a]Degree of stenosis was calculated by NASCET or ECST criteria

to angioscopic images from 9 endarterectomy specimens. Of those, two sections were excluded from analysis due to inadequate histological preparation, and finally 25 histological sections were matched and compared with corresponding angioscopic images.

Histological findings

Table 2 shows results of quantitative histological analysis in the CCA, bifurcation, and ICA. In the present study, plaque rupture was not detected in any histological sections. Vessel and plaque area tended to be larger in the CCA and bifurcation than in the ICA. The absolute necrotic core and IPH area, and fibrous cap thickness were similar among the 3 locations. Similarly, the percent area occupied by the necrotic core and IPH were similar among the 3 locations.

Angioscopic findings

A total of 7 plaques were graded as white plaques, 10 as yellow, and 8 as red by angioscopy. The frequency distribution of white, yellow, and red plaques in each location is shown in Fig. 2. The prevalence of red plaques tended to be lower in the CCA than in the bifurcation and the ICA (22%, 38% and 38%), while yellow plaques were less frequently observed in the ICA than in the bifurcation and the CCA (25%, 38%, and 56%).

Comparison of angioscopic findings and histological parameters

Although vessel and plaque area were similar among the 3 locations, lumen area was smallest in red plaques, followed by yellow and white plaques (8 ± 7 mm^2, 12 ± 7 mm^2, and 20 ± 14 mm^2, respectively, $P = 0.060$). Both the IPH area and the percent area occupied by IPH were significantly larger in red and yellow plaques than in white plaques (10.7 ± 9.3 mm^2, 9.4 ± 7.8 mm^2, and 2.2 ± 1.7 mm^2, respectively, $P = 0.074$, Fig. 3A; and $25 \pm 10\%$, $19 \pm 13\%$, and $7 \pm 5\%$, respectively, $P = 0.008$, Fig. 3B). Similarly, the necrotic core area and the percent area occupied by the necrotic core were largest in red plaques, followed by yellow and white plaques (28.0 ± 18.2 mm^2, 22.2 ± 13.6 mm^2, and 8.5 ± 7.1 mm^2, respectively, $P = 0.038$, Fig. 3C; and $68 \pm 15\%$, $50 \pm 26\%$, and $27 \pm 19\%$, respectively, $P = 0.005$, Fig. 3D). Figure 3E shows the relationship between angioscopic findings and the histological measurement of the fibrous cap thickness. The thickness of the fibrous cap was significantly thinner in red plaques than in yellow and white plaques (128 ± 34 μm, 328 ± 136 μm, and 285 ± 102 μm, respectively, $P = 0.002$). The ROC analysis for predicting a presence of red plaque is shown in Fig. 4. The optimal cutoff value of the fibrous cap thickness for predicting a presence of red plaques was 181 mm, with an area under the curve of 0.987 (100% sensitivity, 90% specificity). Figure 5 shows representative images of angioscopic plaque characterization and their corresponding histology.

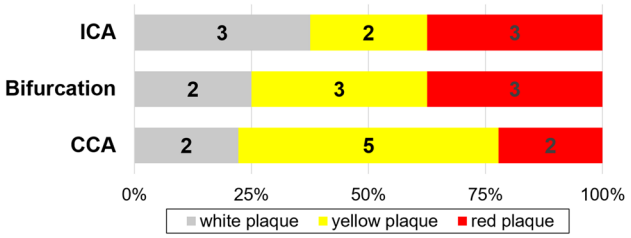

Fig. 2 The frequency distribution of white, yellow, and red plaques in each location (ICA, bifurcation, CCA). There is no statistically significant difference in the distribution of each plaque color among the 3 locations. However, the prevalence of red plaque tended to be lower in the CCA, and the prevalence of yellow plaques tended to be lower in the ICA. *CCA* common carotid artery, *ICA* internal carotid artery

Table 2 Histological analysis among each carotid segment

	CCA (n = 9)	bifurcation (n = 8)	ICA (n = 8)	P value
Minimum lumen diameter (mm)	3.1 ± 1.6	2.5 ± 1.0	1.9 ± 1.5	0.22
Vessel area (mm^2)	57.7 ± 23.5	58.4 ± 25.2	41.5 ± 15.8	0.24
Lumen area (mm^2)	15.9 ± 13.6	13.8 ± 7.0	7.9 ± 9.9	0.24
Plaque area (mm^2)	41.8 ± 20.0	44.6 ± 20.7	33.6 ± 13.7	0.47
IPH area (mm^2)	7.7 ± 9.6	9.1 ± 8.6	6.5 ± 2.9	0.81
Necrotic core area (mm^2)	18.6 ± 18.0	20.3 ± 15.7	22.0 ± 14.0	0.91
Fibrous cap thickness (μm)	228 ± 113	266 ± 154	265 ± 146	0.81
Histological index				
Percent IPH (%)	15 ± 13	19 ± 12	18 ± 13	0.79
Percent necrotic core (%)	43 ± 30	46 ± 25	61 ± 21	0.34

Values are expressed as mean ± SD

CCA common carotid artery, *ICA* internal carotid artery, *IPH* intraplaque hemorrhage

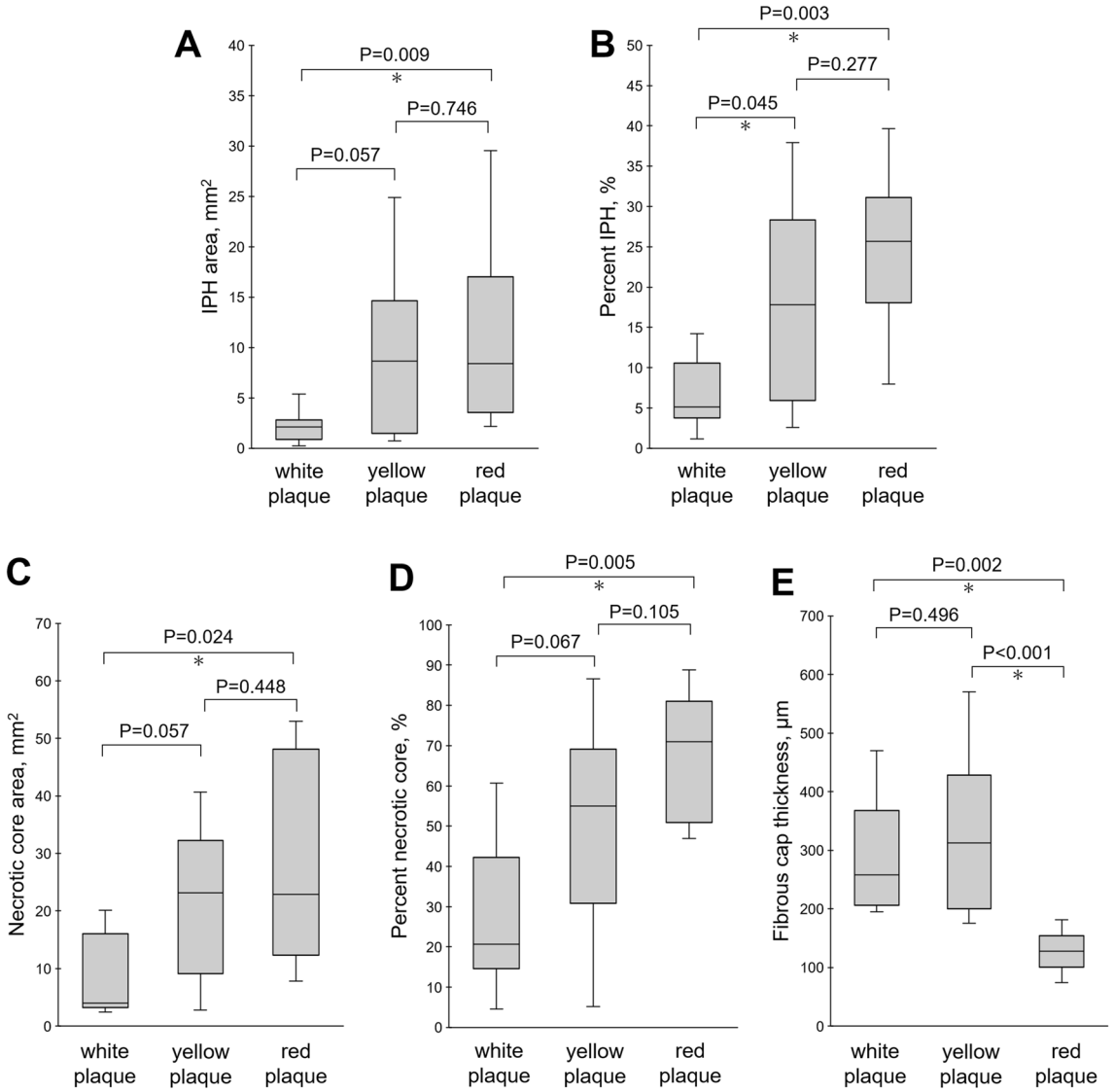

Fig. 3 Comparison of angioscopic findings and histological parameters. **A** The absolute IPH area was larger in both red and yellow plaques than in white plaques (P = 0.03). **B** The percent area occupied by IPH was also larger in red and yellow plaques than in white plaques (P < 0.01). **C** The absolute necrotic core area was larger in red plaques than in yellow and white plaques (P = 0.01). **D** The percent area occupied by a necrotic core was largest in red plaques, followed by yellow and white plaques (P < 0.01). **E** The thickness of the fibrous cap was significantly thinner in red plaques than in yellow and white plaques (P < 0.01). An asterisk indicates a significant difference between the plaques. *IPH* intraplaque hemorrhage

Discussion

The main findings of the present study were as follows: (1) plaques in the carotid artery could be classified as either white, yellow, or red according to the surface color of plaque on angioscopy, (2) IPH area and the necrotic core area was the largest in red plaques, and (3) the thickness of the fibrous cap was thinnest in red plaques. At this time, we believe that this is the first study to demonstrate the capability of angioscopy to identify plaque containing IPH/necrotic core with thin fibrous cap in the carotid artery by ex vivo histological examinations.

In recent years, the operation volume of stent implantation had exceeded CEA due to the improvement of surgical technique. Carotid artery stenting is one of the first choices for the treatment of carotid stenosis together with CEA. However, there are still some concerns regarding the potential higher risk of embolic complication by carotid artery stenting [15]. Therefore, the identification of high-risk plaque for distal embolization and subsequent neurological complications is a major challenge in the field of carotid artery disease. MRI has emerged as a non-invasive imaging modality that enables accurate identification of the components of the atherosclerotic plaque, evaluated by histology

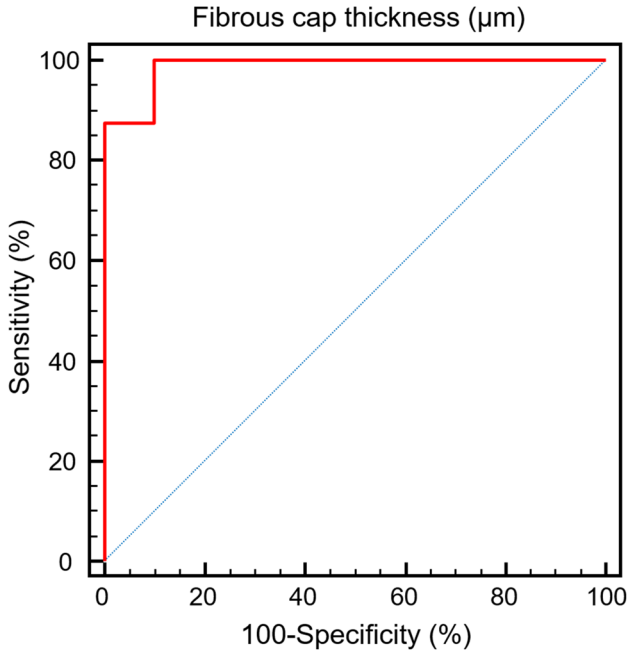

Fig. 4 The receiver operating curve analysis for predicting a presence of red plaque. The optimal cutoff value of fibrous cap thickness was 181 μm (area under the curve = 0.987, 100% sensitivity, 90% specificity)

Fig. 5 Representative images on carotid angioscopy with the corresponding histology. Representative angioscopic image of red plaque (**A**), yellow plaque (**B**), and white plaque (**C**). Corresponding histology of the red plaque has a large necrotic core (a, Hematoxylin-eosin stain, upper image, scale bar = 1 mm; bottom image, scale bar = 200 μm) and a large IPH (b, glycophorin A stain; upper image, scale bar = 1 mm; bottom image, scale bar = 200 μm). The necrotic core area and percent necrotic core area measured 18.4 mm^2 and 82%, respectively. IPH area and percent IPH area were 7.1 mm^2 and 39%, respectively. The fibrous cap thickness calculated 156 μm (c, Masson's trichrome stein; upper image, scale bar = 1 mm; bottom image, scale bar = 100 μm). The corresponding histological image of yellow plaque shows a large necrotic core (d, Hematoxylin-eosin stain, upper image, scale bar = 1 mm; bottom image, scale bar = 100 μm) and IPH (e, glycophorin A stain; upper image, scale bar = 1 mm; bottom image, scale bar = 100 μm). The necrotic core area and percent necrotic core area calculated 29.5 mm^2 and 68% respectively. IPH area and percent IPH area were 16.6 mm^2 and 50%, respectively. The fibrous cap thickness measured 570 μm (f, Masson's trichrome stain; upper image, scale bar = 1 mm; bottom image, scale bar = 500 μm). The corresponding histological image of white plaque showed a small necrotic core (g, Hematoxylin-eosin stain, upper image, scale bar = 1 mm; bottom image, scale bar = 100 μm) and IPH (h, glycophorin A stain; upper image, scale bar = 1 mm; bottom image, scale bar = 100 μm). The necrotic core area and percent necrotic core area calculated as 16.0 mm^2 and 42%, respectively. IPH area and percent IPH area measured 5.4 mm^2 and 29%, respectively. The fibrous cap thickness was 368 μm (i, Masson's trichrome stain; upper image, scale bar = 1 mm; bottom image, scale bar = 200 μm). *IPH* intra plaque hemorrhage, *HE* Hematoxylin-eosin, *MTc* Masson's trichrome

[16]. However, an MRI may still be limited in precise atherosclerotic plaque imaging due to its lower resolution. In addition, it cannot be performed in the catheterization laboratory during diagnostic carotid angiography. Intravascular ultrasound is a catheter-based imaging technique that provides invasive, real time, high-resolution imaging of the carotid plaque. Although an intravascular ultrasound allows for precise and highly reproducible measurements of artery dimensions, it does not have the capability of identifying vulnerable plaques due to its limited axial resolution [17]. Intravascular angioscopy is also a catheter-based imaging modality, which allows for visualization of the morphology of the luminal surface of atherosclerotic plaques, and is widely used. Previous clinical studies reported that angioscopy can identify high risk plaques that may be prone to embolization during stent implantation in the coronary artery [8–10]. The current study showed that carotid plaques could be classified as either white, yellow, or red.

There are two types of angioscopy system available in the current era, non-obstructive angioscopy and occlusion-type angioscopy. Occlusion-type angioscopy needs vessel occlusion by balloon catheter for the removal of blood to clarify the visual field. This is a critical limitation for the clinical use in the coronary artery, because this may cause myocardial ischemia. Non-obstructive angioscopy obtains a visual field by injecting low-molecular-weight dextran into the space between the probing catheter and the fiber. Therefore, non-obstructive angioscopy is relatively safe, because adequate blood flow is maintained throughout the process of image acquisition. Initially this method was used in the coronary artery, and it has since been applied to other larger arteries such as the renal artery and pulmonary artery [8–10, 18, 19]. Likewise, a previous study reported the safety and feasibility of angioscopic observation during carotid angioplasty with stent placement [20]. We believe this imaging technique can be applied to the carotid artery to evaluate plaque morphology. However, it should be noted that there might be some limitations in conducting angioscopic examination in the carotid artery. In some case, angioscopy could not acquire the images of whole vessel wall due to vessel tortuosity and might have missed some plaques. Furthermore, it might be difficult to advance the 2.25Fr angioscopic fiber into a tortuous siphon-like ICA in some case. It should be careful to advance the proving catheter and angioscopic fiber to avoid traumatic dissection, especially in the tortuous artery.

IPH is considered to be caused by rupture of the fragile neovessels formed within the plaque [21]. IPH is thought to be an important atherogenic stimulus by contributing cholesterol to the necrotic core of the plaque and thinning the fibrous cap, thus weakening it and making the plaque

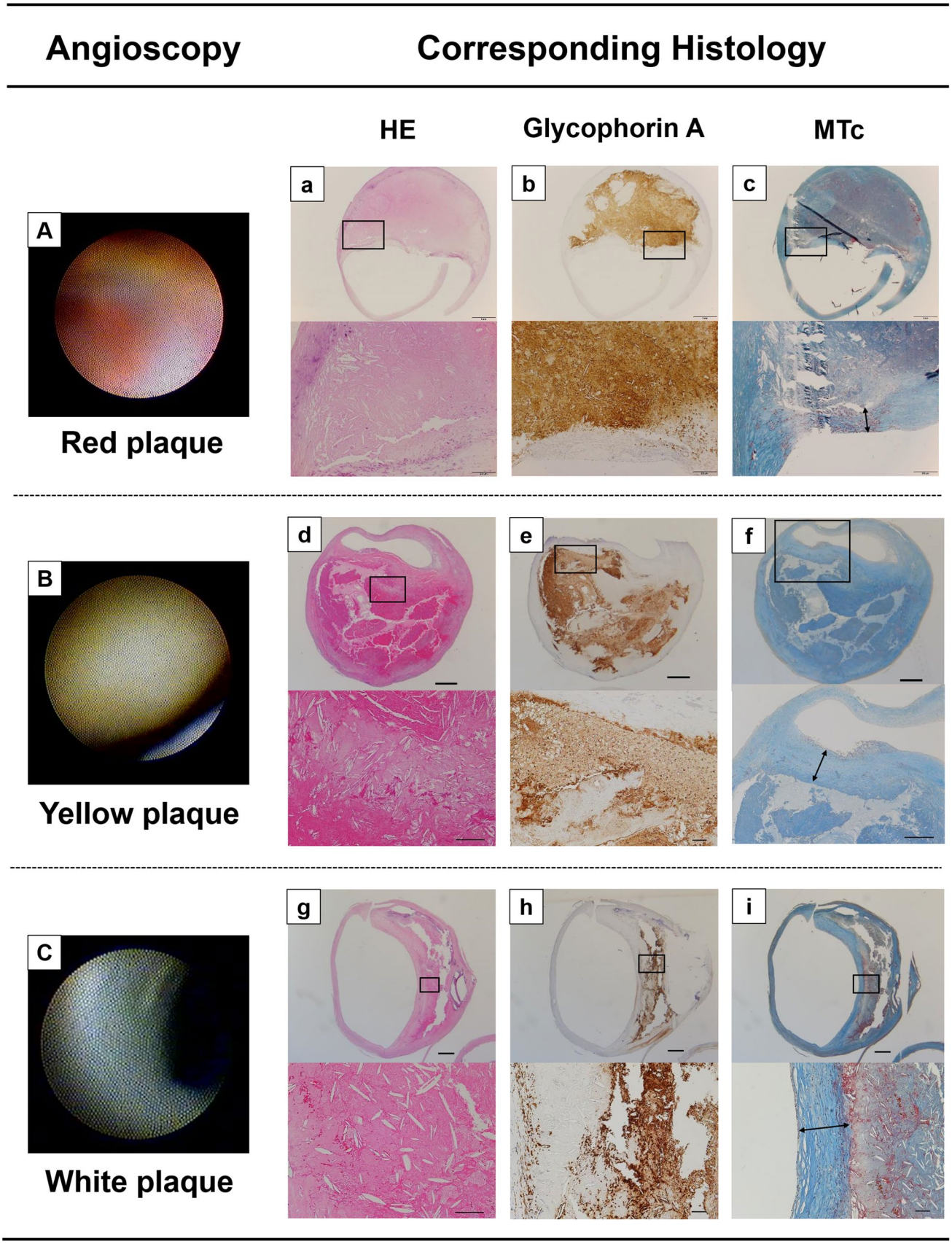
Angioscopy
Corresponding Histology
HE
Glycophorin A
MTc
A
Red plaque
a
b
c
B
Yellow plaque
d
e
f
C
White plaque
g
h
i

more vulnerable [22]. Therefore, the identification of a massive IPH, large necrotic core, and thin fibrous cap may be important to predict plaque rupture and complications during carotid artery stenting. Although an MRI is used to detect IPH with good sensitivity in vivo [23], it is not able to distinguish between IPH and a necrotic core. Moreover, it is still limited in precise fibrous cap imaging due to its lower resolution. Recent studies reported that optical coherence tomography (OCT) has the capability to identify thin fibrous cap because of its high axial resolution [24, 25]. Moreover, OCT can differentiate lipid tissue from fibrous tissue. Because OCT uses near-infrared light and cross-sectional images are generated by measuring the time delay and intensity of light signal that is reflected or backscattered from the arterial wall, OCT has the potential for characterizing tissue morphology by measuring backscattered infrared light. Kume et al has reported that sensitivity and specificity for detecting lipid-rich plaque by OCT was a > 90% in 166 sections from 108 coronary arterial segments of 40 consecutive human cadavers [26]. Lipidic tissue is appeared as low signal intensity regions with diffuse borders because of strong multiple scattering of the OCT light signal at the lipid surface. Therefore, OCT cannot distinguish large necrotic core and small necrotic core. Angioscopy may have an advantage in this respect.

In the present study, we revealed the capability of angioscopy to detect a massive IPH, large necrotic core, and thin fibrous cap by identifying red plaque. The average thickness of the fibrous cap was 128 ± 34 μm for red plaques, which is undetectable by intravascular ultrasound due to its low spatial resolution. The cutoff value of fibrous cap thickness to predict the presence of red plaque on angioscopy was 181 μm with high sensitivity and specificity. A previous histological evaluation of 526 patients undergoing endarterectomy showed that the median cap thickness was 150 μm in ruptured plaques, and the optimum cut-offs for distinguishing between ruptured and non-ruptured plaques was a cap thickness < 200 μm [27]. Moreover, our group has recently demonstrated that 95% of ruptured plaques in the carotid artery had a fibrous cap thickness that was thinner than 130 μm [24]. Therefore, the identification of red plaques by angioscopy in the carotid artery may have benefits in terms of a reduction in not only periprocedural complication, but also future neurological events.

Limitations

This study has several limitations. First, this study was conducted at a single center with a small sample size. Therefore, further investigations must be performed with larger samples to confirm the conclusions. Second, angioscopy in vivo is normally performed under the removal of blood flow by sustained flushing of low molecular dextran. In this study, imaging was conducted under a sustained flush of saline in an ex vivo environment. Third, we have not evaluated quantitative calculation in the longitudinal assessment because pathological sections were not evaluated by longitudinal serial sections. Fourth, the color grades of the plaques were determined visually and unaided, and therefore could be subjective. Finally, only one third of all strokes are caused by thromboembolism from unstable carotid atherosclerotic plaques [28]. It is difficult to predict the other cause of strokes on angioscopy.

Conclusions

The prevalence of red plaques on intravascular angioscopy may represent the existence of plaques containing relatively larger necrotic core and IPH with a thin fibrous cap.

Funding None.

Conflict of interest The authors declare that there is no conflict of interest.

References

1. Timsit SG, Sacco RL, Mohr JP, Foulkes MA, Tatemichi TK, Wolf PA, Price TR, Hier DB (1992) Early clinical differentiation of cerebral infarction from severe atherosclerotic stenosis and cardioembolism. Stroke 23:486–491
2. Petty GW, Brown RD, Whisnant JP, Sicks JD, O'Fallon WM, Wiebers DO (1999) Ischemic stroke subtypes: a population-based study of incidence and risk factors. Stroke 30:2513–2516
3. Palm F, Dos Santos M, Urbanek C, Greulich M, Zimmer K, Safer A, Grau AJ, Becher H (2013) Stroke seasonality associations with subtype, etiology and laboratory results in the Ludwigshafen Stroke Study (LuSSt). Eur J Epidemiol 28:373–381
4. Streifler JY, Eliasziw M, Fox AJ, Benavente OR, Hachinski VC, Ferguson GG, Barnett HJ (1994) Angiographic detection of carotid plaque ulceration. Comparison with surgical observations in a multicenter study. North American Symptomatic Carotid Endarterectomy Trial. Stroke 25:1130–1132
5. Thim T, Hagensen MK, Bentzon JF, Falk E (2008) From vulnerable plaque to atherothrombosis. J Intern Med 263:506–516
6. Takaya N, Yuan C, Chu B, Saam T, Underhill H, Cai J, Tran N, Polissar NL, Isaac C, Ferguson MS, Garden GA, Cramer SC, Maravilla KR, Hashimoto B, Hatsukami TS (2006) Association between carotid plaque characteristics and subsequent ischemic cerebrovascular events: a prospective assessment with MRI–initial results. Stroke 37:818–823
7. Saam T, Hetterich H, Hoffmann V, Yuan C, Dichgans M, Poppert H, Koeppel T, Hoffmann U, Reiser MF, Bamberg F (2013) Meta-analysis and systematic review of the predictive value of carotid plaque hemorrhage on cerebrovascular events by magnetic resonance imaging. J Am Coll Cardiol 62:1081–1091
8. Asakura M, Ueda Y, Yamaguchi O, Adachi T, Hirayama A, Hori M, Kodama K (2001) Extensive development of vulnerable plaques as a pan-coronary process in patients with myocardial infarction: an angioscopic study. J Am Coll Cardiol 37:1284–1288

9. Ohtani T, Ueda Y, Mizote I, Oyabu J, Okada K, Hirayama A, Kodama K (2006) Number of yellow plaques detected in a coronary artery is associated with future risk of acute coronary syndrome: detection of vulnerable patients by angioscopy. J Am Coll Cardiol 47:2194–2200
10. Ueda Y, Matsuo K, Nishimoto Y, Sugihara R, Hirata A, Nemoto T, Okada M, Murakami A, Kashiwase K, Kodama K (2015) In-Stent Yellow Plaque at 1 Year After Implantation Is Associated With Future Event of Very Late Stent Failure: The DESNOTE Study (Detect the Event of Very late Stent Failure From the Drug-Eluting Stent Not Well Covered by Neointima Determined by Angioscopy). JACC Cardiovasc Interv 8:814–821
11. Matsuo K, Ueda Y, Tsujimoto M, Hao H, Nishio M, Hirata A, Asai M, Nemoto T, Murakami A, Kashiwase K, Kodama K (2013) Ruptured plaque and large plaque burden are risks of distal embolisation during percutaneous coronary intervention: evaluation by angioscopy and virtual histology intravascular ultrasound imaging. EuroIntervention 9:235–242
12. Mizote I, Ueda Y, Ohtani T, Shimizu M, Takeda Y, Oka T, Tsujimoto M, Hirayama A, Hori M, Kodama K (2005) Distal protection improved reperfusion and reduced left ventricular dysfunction in patients with acute myocardial infarction who had angioscopically defined ruptured plaque. Circulation 112:1001–1007
13. Barnett HJ, Taylor DW, Eliasziw M, Fox AJ, Ferguson GG, Haynes RB, Rankin RN, Clagett GP, Hachinski VC, Sackett DL, Thorpe KE, Meldrum HE, Spence JD (1998) Benefit of carotid endarterectomy in patients with symptomatic moderate or severe stenosis. North American Symptomatic Carotid Endarterectomy Trial Collaborators. N Engl J Med 339:1415–1425
14. Friedman M, Byers SO, St George S (1962) Origin of lipid and cholesterol in experimental thromboatherosclerosis. J Clin Invest 41:828–841
15. Jaff MR, Goldmakher GV, Lev MH, Romero JM (2008) Imaging of the carotid arteries: the role of duplex ultrasonography, magnetic resonance arteriography, and computerized tomographic arteriography. Vasc Med 13:281–292
16. Yuan C, Mitsumori LM, Ferguson MS, Polissar NL, Echelard D, Ortiz G, Small R, Davies JW, Kerwin WS, Hatsukami TS (2001) In vivo accuracy of multispectral magnetic resonance imaging for identifying lipid-rich necrotic cores and intraplaque hemorrhage in advanced human carotid plaques. Circulation 104:2051–2056
17. Fujii K, Hao H, Shibuya M, Imanaka T, Fukunaga M, Miki K, Tamaru H, Sawada H, Naito Y, Ohyanagi M, Hirota S, Masuyama T (2015) Accuracy of OCT, grayscale IVUS, and their combination for the diagnosis of coronary TCFA: an ex vivo validation study. JACC Cardiovasc Imaging 8:451–460
18. Komatsu S, Ohara T, Takewa M, Takahashi S, Nomamoto T, Kamata T, Nishiuchi K, Kobayashi Y, Kodama K (2014) Nonobstructive angioscopy in patient with atherosclerotic renal artery stenosis. J Cardiol Cases 9:18–21
19. Nakanishi N, Nakamura T, Yamano T, Shiraishi H, Matoba S, Matsumuro A, Shirayama T (2016) Angioscopic observation in chronic thromboembolic pulmonary hypertension before and after balloon pulmonary angioplasty. J Cardiovasc Med (Hagerstown) Dec 17(Suppl 2):e129–e131
20. Tanemura H, Hatazaki S, Asakura F, Kawaguchi K, Kuraishi K, Toma N, Sakaida H, Maeda M, Taki W (2005) Angioscopic observation during carotid angioplasty with stent placement. AJNR Am J Neuroradiol 26:1943–1948
21. Virmani R, Kolodgie FD, Burke AP, Finn AV, Gold HK, Tulenko TN, Wrenn SP, Narula J (2005) Atherosclerotic plaque progression and vulnerability to rupture: angiogenesis as a source of intraplaque hemorrhage. Arterioscler Thromb Vasc Biol 25:2054–2061
22. Kolodgie FD, Gold HK, Burke AP, Fowler DR, Kruth HS, Weber DK, Farb A, Guerrero LJ, Hayase M, Kutys R, Narula J, Finn AV, Virmani R (2003) Intraplaque hemorrhage and progression of coronary atheroma. N Engl J Med 349:2316–2325
23. Bitar R, Moody AR, Leung G, Symons S, Crisp S, Butany J, Rowsell C, Kiss A, Nelson A, Maggisano R (2008) In vivo 3D high-spatial-resolution MR imaging of intraplaque hemorrhage. Radiology 249:259–267
24. Shindo S, Fujii K, Shirakawa M, Uchida K, Enomoto Y, Iwama T, Kawasaki M, Ando Y, Yoshimura S (2015) Morphologic Features of Carotid Plaque Rupture Assessed by Optical Coherence Tomography. AJNR Am J Neuroradiol 36:2140–2146
25. Kini AS1, Vengrenyuk Y, Yoshimura T, Matsumura M, Pena J,, Narula J (2017) Baber U2, Moreno P2, Mehran R2, Maehara A3, Sharma S2. Fibrous Cap Thickness by Optical Coherence Tomography In Vivo. J Am Coll Cardiol 69:644–657
26. Kume T, Akasaka T, Kawamoto T, Watanabe N, Toyota E, Neishi Y, Sukmawan R, Sadahira Y, Yoshida K (2006) Assessment of coronary arterial plaque by optical coherence tomography. Am J Cardiol 97:1172–1175
27. Redgrave JN, Gallagher P, Lovett JK, Rothwell PM (2008) Critical cap thickness and rupture in symptomatic carotid plaques: the oxford plaque study. Stroke 39:1722–1729
28. Barnett HJ, Gunton RW, Eliasziw M, Fleming L, Sharpe B, Gates P, Meldrum H (2000) Causes and severity of ischemic stroke in patients with internal carotid artery stenosis. JAMA 283:1429–1436